Solid State Sciences 13 (2011) 1369–1374

Contents lists available at ScienceDirect

Solid State Sciences

journal homepage: www.elsevier.com/locate/ssscie

The effect of electron irradiation on the electrical characteristics of the Aniline Blue/n-Si/Al device

Şakir Aydoğan [a,*], K. Şerifoğlu [b], Abdulmecit Türüt [a]

[a] Department of Physics, Faculty of Sciences, Atatürk University, 25240 Erzurum, Turkey
[b] Department of Radiation Oncology, Faculty of Medicine, Atatürk University, 25240 Erzurum, Turkey

ARTICLE INFO

Article history:
Received 8 October 2010
Received in revised form
7 March 2011
Accepted 29 March 2011
Available online 3 April 2011

Keywords:
Electron irradiation
Aniline Blue
Schottky barrier
Ideality factor
Series resistance

ABSTRACT

The effect of 12 MeV energy (3×10^{12} e^-/cm^2 fluency) electron irradiation on Au/Aniline Blue(AB)/*n*-Si/Al rectifying device has been studied in terms of the current–voltage (*I–V*), capacitance–voltage (*C–V*), and capacitance–frequency (*C–f*) measurements at room temperature. It has been observed that the electron irradiation causes an increase in the ideality factor and barrier height. The detected changes in *I–V* characteristics have been explained by the formation of radiation-induced point defects. A decrease in the capacitance has been observed after electron irradiation. This has been attributed to a decrease in the net ionized dopant concentration that occurred as a result of electron irradiation.

1. Introduction

Organic semiconductors have attracted increasing interest due to their potential application in various electronic and opto-electronic devices. For example, Schottky contacts have been extensively used to build various organic electronic devices including organic Schottky diodes [1], organic light emitting diodes (OLEDs) [2], and organic solar cells [3]. Schottky contacts obtained by contacting organic semiconductors with metals have been widely used in electronic devices and investigation of the properties of organic semiconductors [4].

The electrical characteristics of a Schottky contact are extremely sensitive to interface state density at the metal–semiconductor interface. It is well known that the interfacial properties of metal/semiconductor (MS) contacts have a dominant influence on device performance, reliability and stability. For this purpose, an organic thin film between metal and inorganic semiconductor can be intentionally made. This film may modify some electrical measurements of the device. The controlled growth of highly ordered thin films either by vacuum deposition or by solution processing is still a subject of ongoing research.

The radiation effects of semiconductor-based devices are very important subjects. The importance of radiation arises from interest in operating semiconductor devices in the industry, space and military applications in a radiation environment, and device fabrication processes such as electron beam deposition, sputtering, ion etching, and ion implantation that expose the device to radiation. In addition, irradiation is a well-established technique used to modify electrical, mechanical and other physical properties of materials in defined regions. Electron irradiation at the interface causes modification of the interface and affects the electrical characteristics of the Schottky diode formed on the semiconductor. Thus, how the contact parameters of the MS contacts give a response to the irradiation can be known. Although various deformation caused by the effects of the radiation have been known, there is not yet a precise explanation of deformation for all types and all parameters of crystals and devices. But in general, the exposure of these devices to high-level particles results in a considerable amount of lattice defects and new electronic states at the inorganic semiconductor–organic material interface. These defects that act as recombination centers or minority/majority carrier trapping centers cause degradation of the diode performance [5–7]. In this work, our purpose is to investigate the effect of electron irradiation on the electrical characteristics of the Au/Aniline Blue (AB)/n-Si/Al device at room temperature.

Aniline Blue (AB) is a mixture of methyl blue and water blue. Furthermore, methyl blue can be used to mediate electron transfer in microbial fuel cells. In this study, Aniline Blue with molecular

* Corresponding author. Tel.: +90 442 231 4073; fax: +90 442 236 0948.
E-mail address: saydogan@atauni.edu.tr (Ş. Aydoğan).

1293-2558/$ – see front matter © 2011 Elsevier Masson SAS. All rights reserved.
doi:10.1016/j.solidstatesciences.2011.03.023

formula $C_{32}H_{25}N_3S_3O_9Na_2$ has been used as an interfacial layer between Au and n-type Silicon. Fig. 1.a and b show the molecular structure of methyl blue and water blue, respectively.

2. Experimental details

We have used a *n*-type Si semiconductor wafer with (1 0 0) orientation and 400 μm thickness and 1–10 Ω cm resistivity. Firstly, the wafer has been subjected to the well known Si cleaning process (i.e. 10 min boiling in $NH_3 + H_2O_2 + 6H_2O$ followed by a 10 min $HCl + H_2O_2 + 6H_2O$ at 60 °C). The ohmic contact has been made by evaporating the Al metal on the back of the *n*-Si substrate, and then it has been annealed at 450 °C for 10 min in N_2 atmosphere. The native oxide on the front surface of the Si has been removed in $HF + 10H_2O$ solution. Finally, it has been rinsed in deionized water for 30 s, and then it has been dried. An AB organic layer (about 200 nm thickness) has been directly formed by simple cast by adding 6 μL of the AB solution (wt. 0.2% in ethanol) to the front surface of the n-Si wafer and dried. Then, Au metal (40 nm thickness) has been evaporated on the AB layer at 10^{-5} torr (diode area = 7.85×10^{-3} cm^2). Eventually, the Au/Aniline Blue/n-Si/Al device has been manufactured. The effects of the 12 MeV energy electron irradiation with an electron fluency of 3×10^{12} e^-/cm^2 on the structure have been investigated. The electrical measurements such as the current–voltage (*I–V*) and capacitance–voltage–frequency (*C–V–f*) have been obtained. The *I–V* measurements have been made by using a KEITHLEY 487 Picoammeter/Voltage Source and the other measurements by using an HP 4192 A (5 Hz–13 MHz) LF IMPEDENCE ANALYZER. There was not any bias voltage applied to the Au/Aniline Blue/n-Si/Al device during the electron irradiation.

3. Results and discussion

The Schottky Barrier Diodes (SBDs) have been characterized by using the thermionic-emission equation given by [8]:

$$I = AA^*T^2 \exp\left(-\frac{q\Phi_b}{kT}\right)\left[\exp\left(\frac{qV}{nkT}\right) - 1\right], \quad (1)$$

where;

$$I_o = AA^*T^2 \exp\left(-\frac{q\Phi_b}{kT}\right), \quad (2)$$

is the saturation current, Φ_b the effective barrier height at zero bias, A^* the Richardson constant which is equal to 112 A/cm^2 K^2 for *n*-type Si. Furthermore, *V* is the applied voltage, *A* is the diode area, and *n* is the ideality factor, introduced to take into account the deviation of the experimental *I–V* data from the ideal thermionic model, given by:

$$n = \frac{q}{kT}\frac{dV}{d(\ln I)} \quad (3)$$

n equals to unity for an ideal diode. However, *n* usually has a value greater than unity. High values of *n* can be attributed to various factors such as the presence of the interfacial thin layer, a wide distribution of low-SBH patches (or barrier inhomogeneities) and the bias voltage dependence of the SBH [8]. Φ_b can be obtained from the following equation:

$$\Phi_b = kT/q \ln\left(AA^*T^2/I_0\right). \quad (4)$$

Fig. 2 depicts the *I–V* characteristics of the Au/AB/n-Si/Al device for unirradiated and irradiated devices. The ratio of forward to

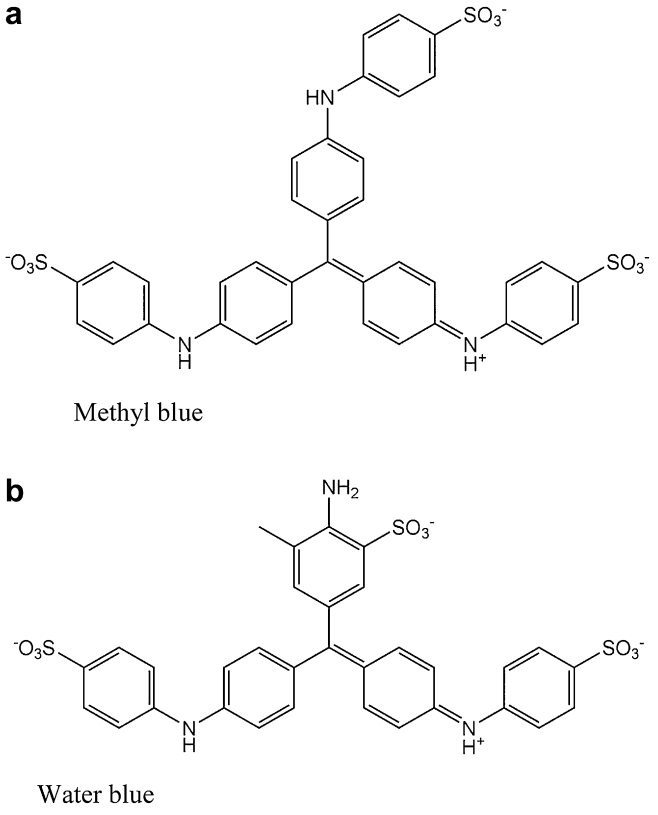

Fig. 1. a The molecular structure of methyl blue b) The molecular structure of water blue.

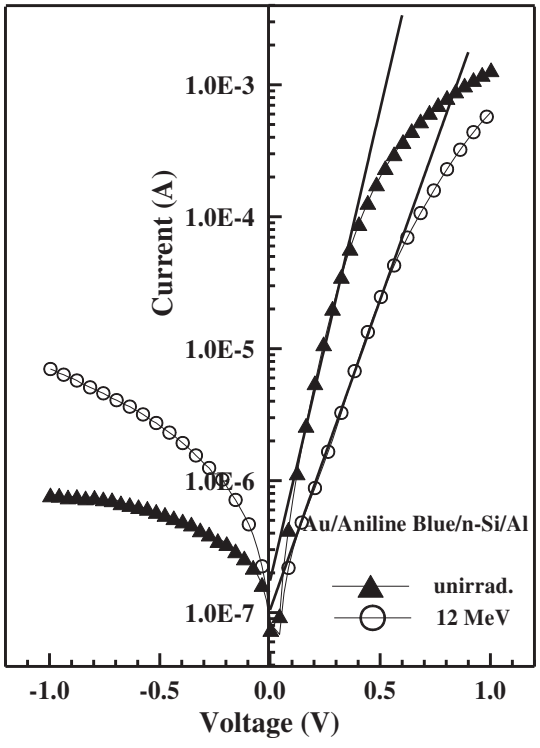

Fig. 2. The forward and reverse bias current–voltage (*I–V*) characteristics of the Au/AB/n-Si/Al device for unirradiated and irradiated with 12 MeV electron energy.

reverse current at a given applied voltage is called *rectification ratio*, and the *I–V* curve of the device shows a well defined rectifying behavior with a rectification ratio as large as 1.6×10^3 at ±1 V for before electron irradiation. It is seen that the *I–V* characteristics of the device have been affected more specifically by the electron irradiation that the saturation current density is found to increase with increasing levels of electron irradiation, which is due to the irradiation induced defects at the interface. Since the defects can be created in the crystal lattice, the defect concentration might increase after irradiation. There are several mechanisms which may be responsible for the change in the *I–V* characteristics after electron irradiation including tunneling, carrier compensation and recombination-generation processes [9]. Thurzo et al. [10] have reported that defects in the surface layer of the semiconductor contribute to a lowering of the rectifying behavior. This behavior may be attributed to an increase in series resistance [11]. Furthermore, the irradiation induced defects at the interface might cause tunneling through the barrier, and in that case the value of the ideality factor increases. The values of the ideality factors for before and after irradiation have been calculated as 2.35 and 3.57, respectively. Furthermore, the high value in the ideality factor is possibly caused by an organic interlayer and by a native oxide film between the top metal (Au) and the silicon. The formation of such a layer is inevitable before deposition of the organic layer on the semiconductor or evaporation of the metal on the organic layer. The values of the barrier heights (BHs) for before and after electron irradiation have been calculated as 0.70 and 0.73 eV, respectively. It has been seen that the value of the SBH has increased with electron irradiation. A modification in the barrier height of the potential barrier is due to the radiation-induced defects at the interface as explained above. The irradiation of materials by high-energy particles is known to introduce lattice defects and the semiconductor properties are sensitive to defect concentrations. Also, the radiation-induced degradation observed in the *I–V* characteristics could be attributed to an increase in interfacial defect density [12–14].

The series resistance is a very important parameter of Schottky diodes and it affects the performance of the devices. Furthermore, an interlayer film between metal and semiconductor may contribute to series resistance. In Au/AB/n-Si/Al device, deposition of AB layer on n-Si may generate a large number of interface states at the semiconductor surface that strongly influence the electrical properties of the device. The forward bias *I–V* characteristics due to thermionic emission of a Schottky contact with series resistance R_S can be analyzed by using Cheung's function [15] defined as;

$$I = I_0 \exp\left[\frac{q(V - IR_s)}{nkT}\right], \tag{5}$$

where the IR_s term is the voltage drop across series resistance of the Schottky diode. The values of the series resistance can be determined from the following functions derived from Eq. (5):

$$\frac{dV}{d(\ln I)} = \frac{nkT}{q} + IR_s, \tag{6}$$

$$H(I) = V - \left(\frac{nkT}{q}\right)\ln\left(\frac{I}{AA^*T^2}\right), \tag{7}$$

and $H(I)$ is given as follows:

$$H(I) = n\Phi_b + IR_s, \tag{8}$$

A plot of $dV/d(\ln I)$ *vs. I* will be linear and gives R_s as the slope and nkT/q as the *y*-axis intercept from Eq. (6). Figs. 3 and 4 show the plots of $dV/d(\ln I)$ and $H(I)$ vs. I for Au/AB/n-Si/Al device. From

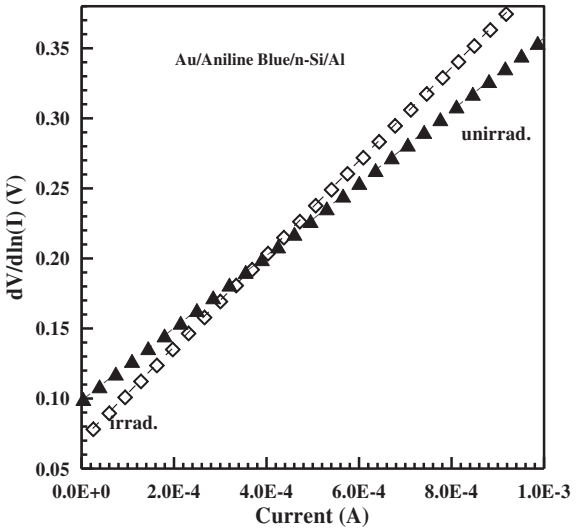

Fig. 3. A plot of $dV/d(\ln I)$ *vs. I* for Au/AB/n-Si/Al device for before and after electron irradiation.

Eq. (6) the values of n and R_s have been calculated as $n = 2.79$, $R_s = 258\ \Omega$ for before and $n = 3.84$, $R_s = 326\ \Omega$, for after electron irradiation. Using the value of the n obtained from Eq. (3), the Φ_b is obtained from the *y*-axis intercept. From $H(I)$ *vs. I* plots, the values of the Φ_b and R_s have been calculated as $\Phi_b = 0.70$ eV, $R_s = 260\ \Omega$ for the pre-irradiation and $\Phi_b = 0.73$ eV, $R_s = 305\ \Omega$, for after 12 MeV electron irradiation. It can be obviously seen that the values of R_s obtained from $H(I)$–I curve are in close agreement with the values obtained from the $dV/d(\ln I)$–I plots. In addition, the series resistance value has slightly increased after 12 MeV electron irradiation.

The value of the series resistance and barrier height can be determined with an alternative method, proposed by Norde [16]: as follows:

$$F(V) = \frac{V}{\gamma} - \frac{kT}{q}\ln\left(\frac{I(V)}{AA^*T^2}\right) \tag{9}$$

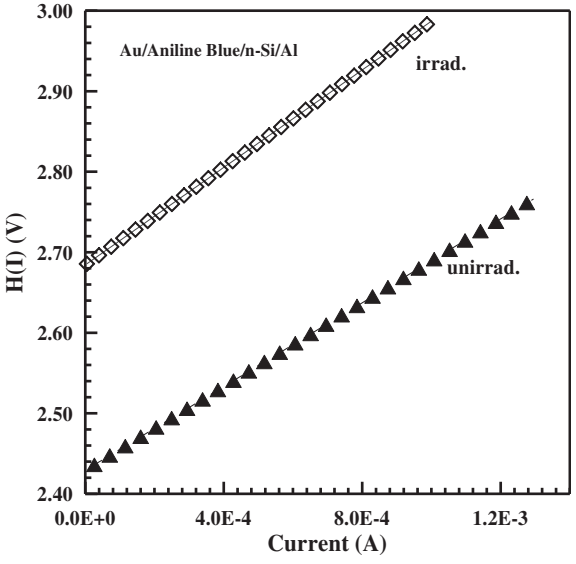

Fig. 4. A plot of $H(I)$ *vs. I* for Au/AB/n-Si/Al device for before and after electron irradiation.

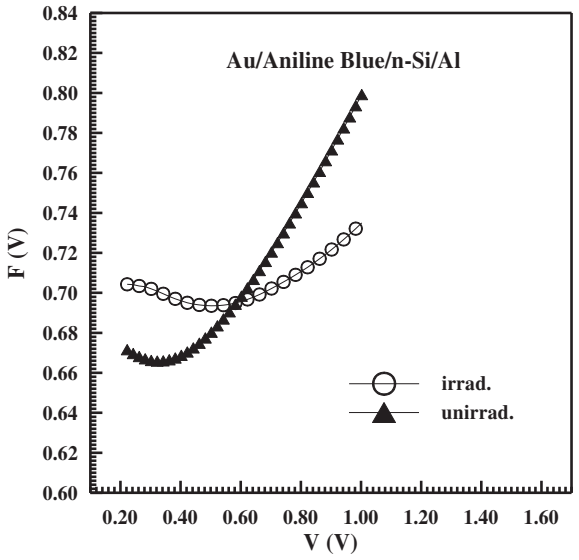

Fig. 5. $F(V)$ vs. V plots of the Au/AB/n-Si/Al device for unirradiated and irradiated case.

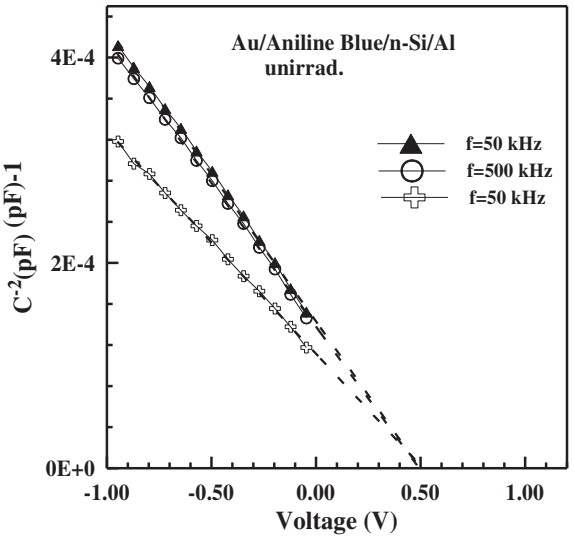

Fig. 7. The reverse bias C^{-2}-V characteristics of the Au/AB/n-Si/Al device before electron irradiation at various frequencies.

where γ is an integer (dimensionless) greater than ideality factor, $I(V)$ is current obtained from the measured I–V plots. From the F vs. V plot the value of barrier height can be obtained by using Eq. (10), where $F(V)$ is the minimum point of $F(V)$ and V_0 the corresponding voltage.

$$\Phi_b = F(V) + \frac{V_0}{\gamma} - \frac{kT}{q} \tag{10}$$

Fig. 5 shows the $F(V)$–V plot of the device. From Norde's functions, R_s value can be determined by using Eq. (11).

$$R_s = \frac{kT(\gamma - n)}{qI} \tag{11}$$

By using Norde's method, the values of series resistance and barrier height have been calculated as 0.74 eV and 259 Ω for the unirradiated and 0.79 eV and 358 Ω for 12 MeV electron irradiation.

It has been seen that the parameters obtained from Cheung functions and Norde's functions agree with each other and both Φ_b and R_s are increased by the applied electron irradiation. An increase in series resistance indicates that the product of the mobility and the free carrier concentration has decreased. The decline in mobility is due to the introduction of defect centers on irradiation which act as scattering centers. The free carrier concentration will decrease if deep traps are introduced into the material associated with point defect displacement damage. Free carriers in the crystal lattice are captured by the defect centers, resulting in decreased carrier density [17].

Figs. 6 and 7 show the C–V plots and reverse bias $1/C^2$ versus V plots of pristine Au/(AB)/n-Si/Al device. In addition, Figs. 8 and 9 show the C–V plots and reverse bias $1/C^2$ versus V plots of irradiated device. It is seen from Figs. 6 and 8 that the values of the capacitance are monotonically increasing toward to the higher voltages and the capacitance in forward biases is sharply increasing.

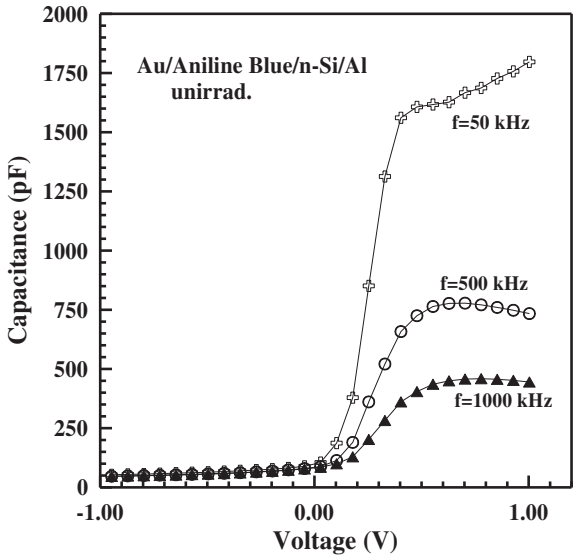

Fig. 6. The forward and reverse bias C–V characteristics of the Au/AB/n-Si/Al device before electron irradiation at various frequencies.

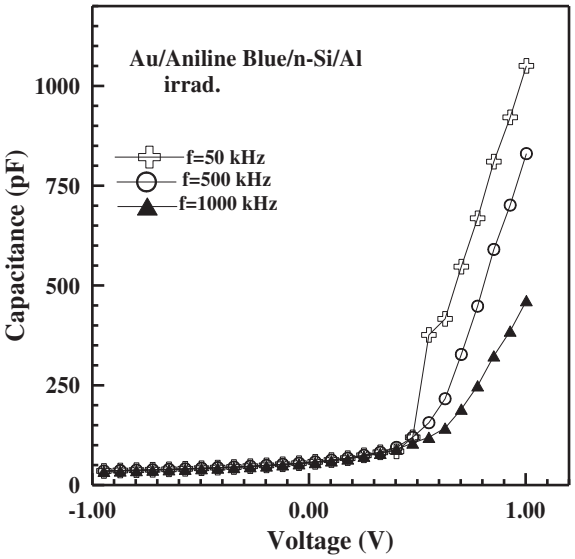

Fig. 8. The forward and reverse bias C–V characteristics of the Au/AB/n-Si/Al device after electron irradiation at various frequencies.

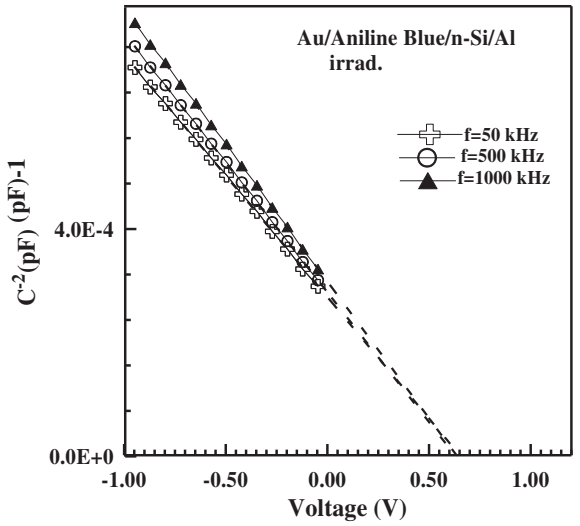

Fig. 9. The reverse bias C^{-2}–V characteristics of the Au/AB/n-Si/Al device after electron irradiation.

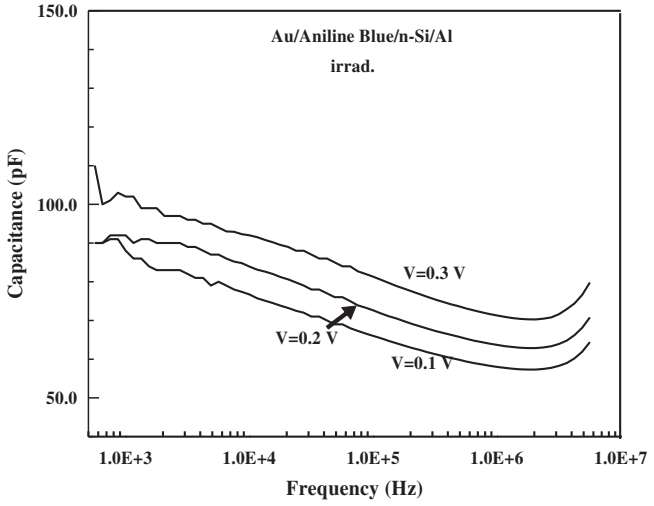

Fig. 11. The forward bias C–f characteristics of the Au/AB/n-Si/Al structure after electron irradiation at various voltages.

The higher values of the capacitance at low frequency are due to the excess capacitance resulting from the interface states in equilibrium with the n-Si which can follow the AC signal. Namely, the interface states at lower frequencies follow the AC signal, whereas at higher frequencies they do not. The values of the capacitance at the high frequency region are only space charge capacitance. From the C–V, the values of the barrier heights were calculated as 0.76 and 0.79 at $f = 500$ kHz for before and after electron irradiation, respectively. The C–V curves gave a Schottky barrier height (BH) value slightly higher than those derived from the I–V measurements. The inhomogeneity has been suggested from the difference between the barrier heights evaluated by I–V and C–V measurements. This difference can be explained by the different nature of the C–V and I–V measurement techniques as well. Barrier heights deduced from two techniques are not always the same. If the barriers are uniform and ideal, the two measurements might yield the same value; otherwise, they will yield different values. The different behavior of BHs obtained from the two techniques can also be explained by a distribution of BHs due to the inhomogeneities (as a combination of the interfacial oxide layer composition, nonuniformity of the interfacial AB layer thickness, and distribution of interfacial charges) that occur at metal/semiconductor interface [18–21]. Furthermore, the increase in barrier height obtained from the C–V characteristics is due to an increase in diffusion potential as shown in Figs. 7 and 9. As a result, an increase for barrier heights can be expected after electron irradiation.

Figs. 10 and 11 depict the capacitance-frequency (C–f) characteristics of Au/(AB)/n-Si/Al device for before and after electron irradiation at various voltages. It is seen from these figures that the capacitance values show a significant decline after electron irradiation. This can be attributed to the change in dielectric constant at the interface, to an increase in the net ionized dopant concentration with electron irradiation or to electron–hole pair generation by the electron irradiation. Any charged particle passing through the semiconductor produces ionization by collisions with electron bound lattice atoms. These collisions excite electrons into the conduction band, leaving behind holes in the valence band. Thus, electron–hole pairs are produced.

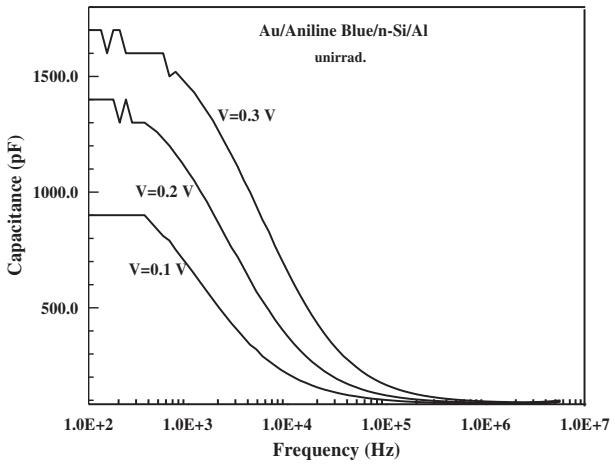

Fig. 10. The forward bias C–f characteristics of the Au/AB/n-Si/Al device before electron irradiation at various voltages.

4. Conclusion

Current–voltage, capacitance–voltage and capacitance–frequency characteristics have been analyzed on the 12 MeV electron irradiated Au/AB/n-Si/Al device. It was seen that the structure with AB layer showed a good rectifying behavior and this means that the charge transport is governed by an additional newly formed AB layer. The I–V measurements show an increase in the change in reverse leakage current after irradiation due to the irradiation induced defects at the interface. Also, it has been seen from capacitance measurements that the capacitance values have decreased after electron irradiation and the values of capacitance are almost independent of frequency up to a certain value of frequency after which the capacitance decreased. The higher values of capacitance at low frequencies have been attributed to the excess capacitance, resulting from the interface states in equilibrium with the n-Si that can follow the AC signal.

Acknowledgments

The authors wish to thank Emrah Tiras ve Alparslan Zora for their contributions.

References

[1] M. Bohm, A. Ullmann, D. Zipperer, A. Knobloch, W.H. Glauert, W. Fix, Printable electronics for polymer RFID applications, presented at ISSCC (2006).
[2] W. Brutting, S. Berleb, A.G. Muckl, Org. Electron. 2 (2001) 1–36.
[3] C.J. Brabec, N.S. Sariciftci, J.C. Hummelen, Adv. Funct. Mater. 1 (2001) 15–26.
[4] A. Takshi, M. Mohammadi, J.D. Madden, Solid-State Electronics 52 (2008) 1717–1721.
[5] M.O. Aboelfotoh, Phys. Rev. B 39 (1989) 5070–5078.
[6] E.H. Nicollian, J.R. Brews, Metal-oxide *Semiconductor Physics and Technology*. Wiley, New Jersey, 1981.
[7] E. Uğurel, Ş Aydoğan, K. Şerifoğlu, A. Türüt, Microelectron. Eng. 85 (2008) 2299–2303.
[8] E.H. Rhoderick, R.H. Williams, Metal-semiconductor Contacts, second ed. Clarendon, Oxford, 1989.
[9] P. Jayavel, K. Santhakumar, J. Kumar, Physica B 315 (2002) 88–95.
[10] I. Thurzo, L. Hrubcin, J. Bartos, E. Pincik, Nucl. Instrum. Methods Phys. Res. B 83 (1993) 145.
[11] G.A. Umana-Membreno, J.M. Dell, G. Parish, B.D. Nener, L. Faraone, U.K. Mishra, IEEE Trans. Electron. Devices 50 (2003) 2326–2334.
[12] V. Baranwal, S. Kumar, A.C. Pandey, D. Kanjilal, J. Alloys Compd. 480 (2009) 962–965.
[13] S.A. Goodman, F.D. Auret, M. Du Plessis, W.E. Meyer, Semicond. Sci. Technol. 14 (1999) 323–326.
[14] O. Güllü, Ş Aydoğan, K. Şerifoğlu, A. Türüt, Nucl. Instrum. Methods Phys. Res. A 593 (2008) 544–549.
[15] S.K. Cheung, N.W. Cheung, Appl. Phys. Lett. 49 (1986) 85–87.
[16] H. Norde, J.Appl. Phys. 50 (1979) 5052–5053.
[17] M. Pattabi, S. Krishnan, S. Ganesh, X. Mathew, Solar Energy 81 (2007) 111–116.
[18] S. Aydogan, M. Saglam, A. Turut, Polymer 46 (2005) 6148–6153.
[19] C. Coskun, Ş Aydogan, H. Efeoglu, Semicond. Sci. Technol. 19 (2004) 242–246.
[20] J. Osvald, E. Burian, Solid State Electronics 42 (1998) 191–195.
[21] S. Kumar, Y.S. Katharria, V. Baranwal, Y. Batra, D. Kanjilal, Appl. Surf. Sci. 254 (2008) 3277–3281.